J Neurosurg 83:271–276, 1995

Magnetic resonance image–directed stereotactic neurosurgery: use of image fusion with computerized tomography to enhance spatial accuracy

EBEN ALEXANDER III, M.D., HANNE M. KOOY, PH.D., MARCEL VAN HERK, PH.D., MARC SCHWARTZ, M.D., PATRICK D. BARNES, M.D., NANCY TARBELL, M.D., ROBERT V. MULKERN, PH.D., EDWARD J. HOLUPKA, PH.D., AND JAY S. LOEFFLER, M.D.

Joint Center for Radiation Therapy and the Stereotactic Radiosurgery and Radiotherapy Program, Departments of Radiation Oncology, Radiology, and Surgery (Neurosurgery), Brigham and Women's Hospital, Children's Hospital, and Harvard Medical School, Boston, Massachusetts

Distortions of the magnetic field, such as those caused by susceptibility artifacts and peripheral magnetic field warping, can limit geometric precision in the use of magnetic resonance (MR) imaging in stereotactic procedures. The authors have routinely found systematic error in MR stereotactic coordinates with a median of 4 mm compared to computerized tomography (CT) coordinates. This error may place critical neural structures in jeopardy in some procedures. A description is given of an image fusion technique that uses a chamfer matching algorithm; the advantages of MR imaging in anatomical definition are combined with the geometric precision of CT, while eliminating most of the anatomical spatial distortion of stereotactic MR imaging.

A stereotactic radiosurgical case is presented in which the use of MR localization alone would have led to both irradiation of vital neural structures outside the desired target volume and underdose of the intended target volume. The image fusion approach allows for the use of MR imaging, combined with stereotactic CT, as a reliable localizing technique for stereotactic neurosurgery and radiosurgery.

KEY WORDS • **stereotactic radiosurgery** • **image fusion** • **stereotaxis** • **magnetic resonance imaging** • **computerized tomography**

STEREOTACTIC localization for operative procedures has become a mainstay of neurosurgical practice. It is most often accomplished with the use of computerized tomography (CT), which, under optimal circumstances, has the advantage of millimeter precision and geometric fidelity. However, CT compares poorly to magnetic resonance (MR) imaging in neuroanatomical definition, most notably in the identification of structures in the brainstem, of nonenhancing lesions, and of anatomically normal structures in functional procedures.[8,9,12,16,22,26] Performed with a stereotactic localizer, MR imaging can yield inaccurate spatial information because of the effect of magnetic susceptibility artifacts and field warping on a patient-peripheral-fiducial system. Stereotactic localization errors are potentially dangerous in the operating room, although other visual cues alert the surgeon to any discrepancy. In noninvasive stereotactic radiosurgery, however, there are no obvious visual checks on stereotactic anatomical precision. The use of radiosurgery doses (1500–2500 cGy) in proximity to critical radiosensitive structures such as the optic chiasm or brainstem mandates a strict appraisal of stereotactic verification when using MR imaging for localization.

In 28 consecutive cases of radiosurgical treatment planning based on both stereotactic MR imaging (using an MR-compatible localizer frame) and stereotactic CT in the same patients, we routinely noted three-dimensional offsets of 3 to 5 mm of MR imaging compared to CT reconstructions, which prompted this particular analysis and solution. After the problem of MR image shift was identified, the treatment volume was often modified to reflect a correction of the discordant MR and CT volumes, but the currently proposed image fusion algorithm is superior in precisely localizing MR-defined structures. A representative case will be presented demonstrating the discrepancy between stereotactic frame MR imaging and CT definition of structures, along with the correction through the image fusion algorithm.

The technique of cross-modality fusion such as MR, CT, single-photon emission computerized tomography (SPECT), and positron emission tomography (PET), combined with the ability to fuse patients' imaging data from

FIG. 1. Coronal, transverse, and sagittal midplane sections through the computerized tomography (CT) and magnetic resonance (MR) volumes before *(upper)* and after *(lower)* the fusion process, demonstrating the CT coordinate system as the reference system. *Upper:* The MR image values are shifted superiorly and to the right compared with the CT bony anatomy. Note the gross misalignment in translation and rotation of the two volumes. The fusion process relies on the automatic segmentation of the surfaces of the bony anatomy in both CT and MR volumes. *Lower:* The bone surfaces from CT are aligned to the bone surfaces in MR using the chamfer matching method described in the text. Note the excellent agreement in the postfusion images between the CT anatomy and the MR anatomy as visualized by the soft-tissue components inside the skull, the bone edges with respect to the MR anatomy, and the sinuses.

time points spread through the course of their illness, provides additional promise for diagnostic radiological evaluation of treatment effects and complications. More sophisticated analysis of imaging data may result from combining and carefully comparing these modalities in stereotactic space, especially when combined with stereotactically directed histological examination.

Clinical Material and Methods

Image Fusion Technique

Image fusion between nonstereotactic MR image and stereotactic CT scan volumes was accomplished by means of the chamfer matching technique described by our group in previous papers.[11,15,25] The computer algorithms involved extracting those voxels that lie at the bone edges of the anatomically complex cranium in both the CT and MR volumes and automating their segmentation and registration with each other.

The MR imaging (without any stereotactic device) was performed on a 1.5-tesla MR imaging system (General Electric Medical Imaging Systems, Milwaukee, WI) using the standard head coil with 5-mm-thick sagittal T_1-weighted images, 3 to 5 mm interleaved contiguous axial proton density T_2-weighted images, and 5-mm interleaved contiguous axial T_1-weighted images postgadolinium. The CT data were acquired on a Somatom Plus CT system (Siemans Medical Systems, Inc., Iselin, NJ) or CT Highlight Advantage 9800 Quick System (General Electric Medical Imaging Systems) using the Brown-Roberts-Wells (BRW) stereotactic localization frame (Radionics, Inc., Burlington, MA) fixed to the patient's scalp. The stereotactic CT scan used 3- to 4-mm-thick contiguous slices.

The first processing step involved the segmentation of those voxels that lie on the surfaces of the bony anatomy in both image sets and identification of their three-dimensional positions (Fig. 1). The segmentation of bone in the CT volume relied on a simple bone threshold, whereas the segmentation in MR volume relied on a spectral analysis of voxel values;[25] both are automatic and rapid. The MR volume was subsequently transformed in the following manner: all voxels identified as bone-surface voxels were assigned the value of 0, and all other voxel values were replaced with a value denoting the closest distance of the voxel to a bone surface.[11,24] This transformation represented a distance transform of the original MR image volume, and the distance-transformed MR volume formed the template or chamfer for the match.[1,2]

FIG. 2. Illustrative case. *Left:* Gadolinium-enhanced stereotactic T_1-weighted axial magnetic resonance (MR) image revealing a left acoustic neurinoma, obtained with the MR–fiducial rod localizer in place. The orange-filled contour indicates the intended 80% isodose surface for the radiosurgical treatment (80% = 1500 cGy) and includes the entire tumor. *Center:* Axial bone window stereotactic computerized tomography (CT) scan indicating the same 80% isodose contour (in orange) as it relates to the internal auditory canal. *Right:* An axial image fusion MR image (the small white dots represent bone edges from the CT scan used to fuse the image with the bone visualized on MR) showing that the true isodose contour is displaced posteriorly by 4 mm compared with the original stereotactic MR image. This image distortion would have led to unrecognized dose distribution into the anterolateral pons and middle cerebellar peduncle, leaving the anterior aspect of the tumor undertreated. Note that fiducial rods from both CT and MR frames are reproduced.

If a bone voxel identified on CT was placed in the MR imaging volume at the location given by the CT voxel coordinate, an MR voxel and value would be found that denoted the distance from the CT voxel to the closest MR bone edge. If the CT and MR imaging were perfectly aligned and the segmentation were ideal, this value would equal zero. All CT voxels were then considered and an attempt was made to minimize the sum of all distances obtained in the MR image volume by applying the transformation operations of translation, rotation, and scaling between the CT and MR coordinate systems. The transformation that minimized the overall sum of distances was presumed to be the best alignment between the two volume sets.[4,15,17] Using a Monte Carlo technique to vary parameters around the initially assumed model of a "true" image match, a mean cost function combined with a Downhill Simplex optimization procedure yielded the lowest number of false positives (1.8%). Accuracy was better than 1 mm and the capture range for the two coordinate systems was less than 6 cm.[25]

Results

The actual matching procedure described above was very rapid and took approximately 30 seconds on current HP 9000/755 workstations (Hewlett-Packard, Inc., Palo Alto, CA). The accuracy of the match was verified for each patient and involved a detailed comparison along arbitrary planar reconstructions (coronal, axial, and sagittal sections) for the alignment of the internal anatomy. If the match was not sufficiently accurate, the procedure allowed an optimization of the parameters of the segmentation process to minimize the discrepancy.

The fusion resulted in the alignment of the nonstereotactic MR image volume to the stereotactic CT scan volume. The CT volume allowed a first-order calibration of the distortion effects in the MR image for a patient. The correction did not rely on external calibrations or statistical inferences based on phantoms. The fusion created a new data set from the original stereotactic CT volume and replaced the CT pixel value with the MR pixel value at that location. Thus, this new data set was an MR imaging data set that used the distortion-free CT stereotactic fiducial markers to achieve stereotactic localization.

The quality of fit of the final image fusion data set could be demonstrated with many soft tissue and bone features. Our software allowed creation of a small window that could be rapidly moved around on the CT planar image to show the corresponding MR image and demonstrate goodness-of-fit of any anatomical structures. The quality assurance protocol depended on this comparison between stereotactic CT and the fused MR data that were acquired. In general, image shifts of greater than 1 mm were seen only at the tissue–air interface. Stereotactic CT–MR image fusion for localization of external surface features on a patient therefore yielded an unsatisfactory result.

Illustrative Case

This 59-year-old woman presented with progressive hearing loss over 2 years due to an acoustic neurinoma and was selected for treatment with radiosurgery. Axial MR images with the stereotactic localizer ring in place demonstrated displacement of the MR tumor image posteriorly, directly into the anterolateral brainstem (Fig. 2). Dose–volume histogram analysis of both treatment plans (using the MR stereotactic frame and MR image fusion) was reviewed. Based on the plan of the MR stereotactic frame–defined tumor, 100% of the tumor volume was covered by 80% of the total dose (prescribed as 1500 cGy to the 80% isodose surface). However, because of the 4-mm posterior displacement of the 0.96 cc target volume demonstrated via image fusion, only 83% (0.80 cc) of the actual tumor volume was covered by the prescribed dose.

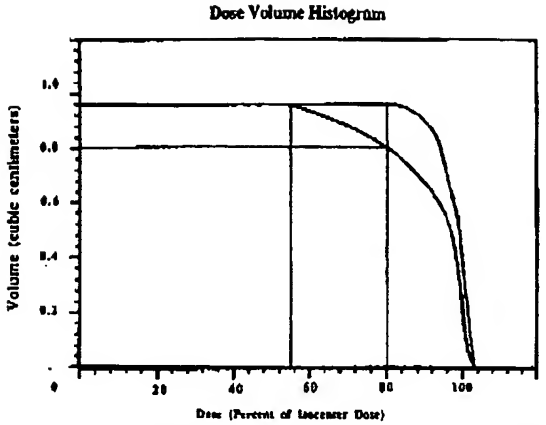

FIG. 3. Dose–volume histogram (DVH) from the case illustrated in Fig. 2. The curve on the right (with the steepest shoulder) is the intended DVH, with the typical steep shoulder for a single isocenter radiosurgical case with minimum tumor dose inhomogeneity and complete tumor coverage. The right vertical line indicates the minimum peripheral tumor dose (1500 cGy) prescribed to the 80% isodose distribution. The left curve (with a more gradual shoulder) indicates the actual treatment DVH, with the vertical line indicating the 55% isodose distribution (not the 80%) receiving the prescribed dose. This resulted in 0.80 cc of the 0.96-cc tumor volume (83%) receiving the intended 1500 cGy, leaving 17% of the tumor volume (the anterior aspect shown in Fig. 2 *right*) exposed to a potentially subtherapeutic dose.

The anterior 17% of the tumor volume, therefore, would receive less than the prescribed dose if the image fusion correction was not made (Fig. 3). Without appropriate correction for this MR image distortion, the dose to the anterolateral pons and cerebellar peduncle would be greater than expected.

Discussion

Imaging studies in which spatial relations are quantitatively accurate are a prerequisite for modern stereotactic techniques. Because data acquisition with CT scanning was obtained via x-ray photons, whose paths are not subject to measurable deflection by the elements involved in producing an image, distortion is inconsequential with a still subject.[9,19] The magnetic fields produced within the MR imager, on the other hand, are not necessarily free of such influences. For diagnostic imaging this is not a problem because the primary concerns are the relationships between adjacent structures. For imaging in conjunction with stereotactic procedures, comparisons are made between distant structures, and the reliability of MR imaging for this application has been questioned.[8,10,19]

An MR localization in combination with a stereotactic frame relies on fiducial markers, calibrated with respect to the frame, which are imaged with the patient.[5] These fiducial markers are used to generate a transformation from the image-modality coordinate system to the stereotactic coordinate system. Stereotactic localization based on CT is a highly accurate procedure with millimeter range accuracy, in optimum circumstances. An MR image often provides superior anatomical definition of intracranial targets compared with CT, but suffers from spatial distortion secondary to magnetic field warping, susceptibility artifacts, and chemical shift effects.

Stereotactic localization using MR imaging suffers from lack of geometric fidelity in the reconstructed images. The manufacturer, in fact, advises against the use of MR imaging for applications demanding geometric precision, and states that the overall accuracy is 2% of the field-of-view (Radionics, Inc.: personal communication, 1994).

Some reports claim that distortion of MR images is not significant in stereotactic localization, whereas others report linear distortions on the order of 4 mm.[14,23] A recent study by Kondziolka, *et al.*,[14] concluded that the magnitude of MR image distortion was less than one pixel on accompanying CT scans and was thus insignificant. Other studies have reported significant errors, as great as 5 mm on average, between MR and CT images.[3,10,23,26]

In our experience with 28 radiosurgery patients analyzed simultaneously with both stereotactic CT and stereotactic (frame-based) MR imaging, three-dimensional distortions of 4 mm (median range 3 to 5 mm) were noted. The MR displacement was in a posterior direction on axial images and a superior direction on coronal images.

Radiosurgery offers significant benefit by enabling dose gradients from 80% to 10% (of maximum dose) over approximately 6 to 8 mm. Given that the primary indication for the addition of MR imaging to CT scans in these radiosurgery cases was proximity of the lesion to the optic chiasm (the most radiosensitive of intracranial structures), this amount of spatial discrepancy was quite alarming. Our images of phantoms also consistently showed gross misalignment of fiducial rods with MR imaging.[15]

A number of factors may contribute to the inhomogeneity of the magnetic field and, thus, to distortion in the MR image. Fluctuations in power supply or temperature and the placement of ferromagnetic structures in the vicinity of the magnet can affect the geometry of the magnetic field.[6,7] Susceptibility artifacts at air–water and air–fat interfaces lead to unavoidable spatial distortions. Magnetic susceptibility artifacts are of greatest concern in the imaging of fiducial rods, because they have sharp material interfaces and are located far from the center of the magnetic field in which field warping is greatest.[7,19] The air–rod interface can lead to significant susceptibility artifact with rod distortion and, therefore, alterations in the three-dimensional coordinate system used to define anatomical localization.

Another source of artifact is the chemical shift–induced spatial misregistration between water and lipid signals. The use of petrolatum for rod material, although useful for generating a strong signal in typical imaging schemes, introduces further spatial misregistration because of chemical shift effects. In routine MR imaging, the chemical shift differences between protons bonded to carbon, as in fat and petroleum gels, and protons bonded to oxygen, as in water, lead to spatial displacements between these two materials in both the frequency-encoding dimension and the slice-selection dimension.[27] In brief, the intrinsic and extrinsic mechanisms of spatial distortion in MR imaging are numerous and difficult to account for quantitatively.

Despite these difficulties, MR imaging remains an important and attractive modality for stereotactic procedures. Potential image distortion, with greater cost and scanning time and less accessibility, are often outweighed by the increased resolution afforded by MR imaging. Stereotactic MR imaging is often necessary, particularly with biopsies of small, poorly enhancing, or deep lesions or in certain functional neurosurgical procedures.[8,9,12,16,22]

Image fusion is a technique that combines often complementary information from two or more separate imaging studies into a single consistent imaging study. There are two commonly used image-fusion techniques. The first is based on systems of fiducial markers, in which markers visible with both modalities can be used to align the two images.[21] This method relies on only a small number of data points, which inherently reduces its precision. The second is based on surface matching between volumes identified in both techniques.[13,18]

Our group has described a method of image fusion between MR and CT via a chamfer matching technique that has been used extensively for radiosurgery.[15] This technique involves the automated matching of the sets of points consisting of the surface of the skull in MR images and CT scans (Fig. 3). In this method, the MR data from inside the skull are effectively combined with the spatially accurate stereotactic CT data: the resolving power of MR imaging can be applied in conjunction with the fiducial accuracy and reliability of CT. Furthermore, in many cases the CT image can be used to verify points chosen with MR. The method is very robust against partial volume effects and uses the full volumetric information to rapidly fuse the image sets. It provides an interactive quality-assurance procedure to verify the accuracy of the fusion on a per patient basis, and it relies on resampling both images in a uniform coordinate system, allowing arbitrary plane reconstruction. Obvious landmarks include the major arteries, ventricular spaces, and bone demarcations.

Using the chamfer technique, the point of interest can be localized to the skull with MR imaging, and the skull can be localized to fiducial rods with CT, thus eliminating the effects of an MR artifact where it is greatest. We have used this technique in operative stereotactic procedures (both surgical and radiosurgical), thus minimizing MR spatial artifacts in cases in which this imaging modality is necessary.

The fusion process is dependent on calculations using an up-to-date computer workstation; computing time for completion of an image fusion is approximately 2 minutes using our workstation. Much more time is spent verifying the accuracy of the fused image, which involves expert evaluation of the results along three planes. Verification time is generally expected to be less than 1 hour.[15]

As stated above, most of the image distortion involved with stereotactic MR can be expected along the fiducial rods, because of their peripheral location and effects at the air–rod interface. Rousseau, *et al.*,[20] described a method in which four fiducial markers are attached directly to the skull. Because of the small number of referential points, error in target selection may actually be increased using this method; in addition, the air–skin or air–surface marker interface is highly susceptible to distortions. Chamfer matching offers a statistical matching of 5000 to 10,000 separate MR-defined points on the skull for mapping into the stereotactic CT spatial dataset.

Summary

We have presented an example of image fusion using the chamfer technique in operative neurosurgery. For the last 3 years, all MR-guided procedures performed in our center have used image fusion of MR with stereotactic CT via this method, yielding more precise stereotactic localization of anatomical structures. For MR-guided neurosurgical and radiosurgical procedures in which spatial localization accuracy of less than 5 mm is mandatory, image fusion offers an elegant solution.

References

1. Barrow HG, Tenenbaum JM, Bolles RC, et al: Parametric correspondence and chamfer matching, in **Proc 5th Int Joint Conf on Artificial Intelligence**. Cambridge, MA. 1977, pp 659–663
2. Borgefors G: Hierarchical chamfer matching: a parametric edge matching algorithm. **IEEE Trans Pattern Recogn Machine Intell 10**:849–865, 1988
3. Bradford R, Thomas DGT, Bydder GM: MRI-directed stereotactic biopsy of cerebral lesions. **Acta Neurochir (Suppl) 39**: 25–27, 1987
4. Brent RP: **Algorithms for Minimization Without Derivatives**. Englewood Cliffs, NJ: Prentice Hall, 1973
5. Brown RA, Roberts TS, Osborn AG: Simplified CT-guided stereotaxic biopsy. **AJNR 2**:181–184, 1981
6. Harpen MD: Magnetically induced surface charges on samples in magnetic resonance imaging radio-frequency coils: effect on electric fields, sample losses, and coil resonance. **Med Phys 17**:362–368, 1990
7. Harris R, Wesbey G: Artifacts in magnetic resonance imaging, in Kressel HY (ed): **Magnetic Resonance Annual 1988**. New York: Raven Press, 1988, pp 71–112
8. Hassenbusch SJ, Pillay PK, Barnett GH: Radiofrequency cingulotomy for intractable cancer pain using stereotaxis guided by magnetic resonance imaging. **Neurosurgery 27**:220–223, 1990
9. Heilbrun MP: Image-guided stereotactic surgery: adjunct technical advances, in Wilkins RH, Rengachary SS (eds): **Neurosurgery Update II**. New York: McGraw-Hill, 1991, pp 373–378
10. Heilbrun MP, Sunderland PM, McDonald PR, et al: Brown-Roberts-Wells stereotactic frame modifications to accomplish magnetic resonance imaging guidance in three planes. **Appl Neurophysiol 50**:143–152, 1987
11. Hongjian J, Robb RA, Holton K: A new approach to 3D registration of multimodality medical images by surface matching, in Robb RA (ed): **Visualization in Biomedical Computing. Proc SPIE 1808**:197–213, 1992
12. Kall BA: Computer and imaging technology's impact on stereotactic neurosurgery. A 1989–1991 update. **Stereotact Funct Neurosurg 58**:90–93, 1992
13. Kessler L, Pitluck S, Petti P, et al: Integration of multimodality imaging data for radiotherapy treatment planning. **Int J Radiat Oncol Biol Phys 21**:1653–1667, 1991
14. Kondziolka D, Dempsey PK, Lunsford LD, et al: A comparison between magnetic resonance imaging and computed tomography for stereotactic coordinate determination. **Neurosurgery 30**:402–407, 1992
15. Kooy HM, van Herk M, Barnes PD, et al: Image fusion for stereotactic radiotherapy and radiosurgery treatment planning. **Int J Radiat Oncol Biol Phys 28**:1229–1234, 1994

16. Lunsford LD: Magnetic resonance imaging stereotactic thalamotomy: report of a case with comparison to computed tomography. **Neurosurgery 23:363–367, 1988**
17. Nelder JA, Mead R: A simplex method for function minimization. **Comput J 7:308–313, 1965**
18. Pellazari CA, Chen GTY: **The Use of Computers in Radiation Therapy.** North Holland: Elsevier, 1987, pp 437–440
19. Peters TM, Clark J, Pike B, et al: Stereotactic surgical planning with magnetic resonance imaging, digital subtraction angiography and computed tomography. **Appl Neurophysiol 50: 33–38. 1987**
20. Rousseau J, Clarysse P, Blond S, et al: Validation of a new method for stereotactic localization using MR imaging. **J Comput Assist Tomogr 15:291–296, 1991**
21. Schad LR, Boesecke R, Schlegel W, et al: Three dimensional image correlation of CT, MR, and PET studies in radiotherapy treatment planning of brain tumors. **J Comput Assist Tomogr 11:948–954. 1987**
22. Thomas DGT, Davis CH, Ingram S, et al: Stereotaxic biopsy of the brain under MR imaging control. **AJNR 7:161–163, 1986**
23. Tien RD, Buxton RB, Schwaighofer BW, et al: Quantitation of structural distortion of the cervical neural foramina in gradient-echo MR imaging. **J Magn Reson Imag 1:683–687, 1991**
24. van Herk M: A fast algorithm for local minimum and maximum filters on rectangular and octangular kernels. **Pattern Recogn Lett 13:517–521, 1992**
25. van Herk M, Kooy HM: Automatic three-dimensional correlation of CT-CT, CT-MR, and CT-SPECT using chamfer matching. **Med Physics 21:1163–1178, 1994**
26. Villemure JG, Marchand E, Peters T, et al: Magnetic resonance imaging stereotaxy: recognition and utilization of the commissures. **Appl Neurophysiol 50:57–62, 1987**
27. Wachsberg RH, Mitchell DG, Rifkin MD, et al: Chemical shift artifact along the section-select axis. **J Magn Reson Imag 2: 589–591, 1992**

Manuscript received June 3, 1994.
Accepted in final form October 24, 1994.

Address reprint requests to: Eben Alexander III, M.D., Department of Neurosurgery, Brigham and Women's Hospital, 75 Francis Street, Boston, Massachusetts 02115.